Transition-metal impurities in dilute $Fe_{3-x}T_xSi$ alloys: A spin-echo NMR investigation

T. J. Burch
Marquette University, Milwaukee, Wisconsin 53233

J. I. Budnick
University of Connecticut, Storrs, Connecticut 06268

V. A. Niculescu
Virginia Commonwealth University, Richmond, Virginia 23284

K. Raj
Ferrofluidics Corporation, 40 Simon Street, Nashua, New Hampshire 03061

T. Litrenta
Computer Signal Processors Inc., 40 Linnell Circle, Billerica, Massachusetts 01821
(Received 14 October 1980; revised manuscript received 11 May 1981)

A comprehensive collection of spin-echo NMR spectra from nuclei of both host and transition-metal impurities (T) in pseudobinary $Fe_{3-x}T_xSi$ alloys taken at about 1.3 K are presented and analyzed. We summarize some new data on $3d$ elements and also review briefly some results already reported. Previously unpublished results for $4d$ and $5d$ elements are reported. Fe_3Si has two inequivalent Fe sites and one Si site. From the analysis of the solute spectra we show that the $3d$, $4d$, and $5d$ elements under Fe or to the right of Fe in the periodic table (Ni, Co, Ru, Pd, Os, and Ir) enter the Fe site with four Fe and four Si first neighbors. The $3d$ elements to the left of Fe (Mn, V, Cr, and Ti) enter the Fe site which has eight Fe first neighbors. In addition, we report that in Fe-rich nonstoichiometric alloys Ni, Ru, Rh, and Pd prefer A,C sites with the smallest number of Fe first neighbors. The roles of electronic structure, electronegativity, and atomic size in producing the observed selectivity are analyzed. Finally a comparison between impurity hyperfine fields in Fe_3Si and Fe, Ni, and Co hosts is made. The dependence of impurity hyperfine fields on both the moment of the host and the position of the impurity in the periodic table, found for Fe, Ni, and Co hosts, are also shown to exist in the case of Fe_3Si alloys. Using these dependences, we make tentative predictions of the fields at some nuclei for which spectra were not observed.

I. INTRODUCTION

A major area of theoretical and experimental interest in both magnetism and alloy physics is the determination of the role that local atomic environments play in chemical and magnetic interactions. In ferromagnetic alloys the magnitude and distribution of the hyperfine fields at the nuclei are produced by the electrons of the atom itself and conduction electrons and thus are generally sensitive to slight changes in an atom's local magnetic and crystalline environment. Thus, analysis of NMR or Mössbauer spectra, which measure internal fields versus the number of nuclei seeing that field, can yield information about the bonding mechanisms, valency states, and long- and short-range exchange interactions of the ions involved.

Analysis of the extensive data on host and transition element impurity hyperfine fields in the dilute binary alloys of Fe, Ni, and Co has, for the most part, been based on phenomenological models. In these models the changes in the fields at a given site near an impurity are usually attributed to: (1) a change in the local d moment on the atomic site owing directly to neighboring impurities and (2) to a change in the conduction-electron polarization contribution to the hyperfine field due to moment changes of neighboring sites. In binary alloys with a random distribution of impurities the complex spectra, which are sums of overlapping contributions from nuclei with a large number of different near-neighbor configurations, makes it difficult to separate the contributions of any one site. The difficulty of separating the on-site contributions from the contribution of neighboring atoms is even greater.

The ferromagnet Fe_3Si is a long-range crystallo-

graphically ordered alloy with the DO_3 structure, an order parameter near 1 and two well-defined Fe sites. The pattern of site occupation is readily described both in nonstoichiometric alloys and alloys formed by transition-metal substitutions.[1-3] Indeed, transition-metal impurities enter only one of the two Fe sites. This preferential occupation of Fe sites by these impurities not only simplifies the NMR spectra but is an important result in its own right.

Because of their relatively simple crystallographic and magnetic properties, Fe_3Si and its pseudobinary transition-metal alloys offer a limited number of relatively well-defined sites with near-neighbor configurations and atomic moments which change in predictable ways with alloy composition. In the most favorable cases analysis of the concentration dependence of NMR spectra have yielded separations of the on-site contributions to hyperfine fields from those of neighboring atoms.

In this paper NMR spectra at the matrix sites and at the substitutional transition-metal (T) sites in a large number of pseudobinary systems $Fe_{3-x}T_xSi$, in dilute concentration ranges are presented. From this NMR data conclusions are drawn about the selective properties of impurity substitutions. From the solute spectra it is shown that $3d$, $4d$, and $5d$ elements under or to the right of Fe in the periodic table all enter the Fe sites, which have four Fe and four Si first near neighbors [Fe(B)]. In nonstoichiometric pseudobinary alloys, where Fe(A,C) sites with different numbers of Fe first neighbors occur, the preference of some impurities for the sites with fewest Fe neighbors is reported and discussed. The similarity of transition-metal-substituted Fe_3Si alloys to the Heusler alloys, a class of ferromagnetic alloys on which extensive experimental and theoretical work exists, is pointed out and analyzed. The roles of electronic structure, atomic size, and electronegativity as determinants of the observed selectivity are explored. Finally, the hyperfine fields at transition-metal atoms substituted in the Fe_3Si matrix are compared with the fields of transition-metal impurities in Fe, Ni, and Co hosts.

II. SAMPLE PREPARATION AND ANALYSIS

Appropriate amounts of high-purity (99.999%) materials were arc melted in an argon atmosphere. The weight loss during melting was less than 0.5% for all samples. Most of the samples discussed here were prepared from the ingots by crushing and powdering to No. 100 mesh, annealing at about 550 °C for 1 h under vacuum to relieve strain, and then cooling at a rate of about 10 °C/min. In the cases of V, Mn, and Co alloys a more elaborate procedure, which produced a high degree of long-range order in alloys with large x, was adopted.[4,5] Before powdering to No. 400 mesh and relieving strain, these alloys were sealed in quartz under a vacuum of about 10^{-6} Torr, annealed at 800 °C for 24 h, cooled from 800 to 600 °C at a rate of about 40 °C/h, and then water quenched. The smaller particle size was used to reduce the effects of skin depth on the experimental results and thus enhance the NMR signal strength.

An x-ray-diffraction powder pattern using Cu $K\alpha$ radiation was obtained for each sample at room temperature. The procedure used and the method of analysis have been discussed elsewhere.[4] Single-phase materials with clear superlattice lines for the DO_3 structure were obtained for alloys with Ti, V, Cr, Mn, Co, Ni, Ru, Rh, Os, and Ir substitutions. The lattice constant of Fe_3Si is 5.6539 Å. The addition of Co decreases this lattice parameter while additions of Mn, V, Cr, Ti, Ru, and Rh increase it. Materials formed from substitutions of Sc, Cu, Nb, Mo, Pd, Ag, Hf, Ta, W, Pt, and Au were not of a single phase. No extensive study of the effects of heat treatment on the degree of long-range order or on the formation of second phases were attempted for the low-concentration samples described in this paper. Limited attempts were made to produce single-phase materials by quenching and or varying annealing times and temperatures for only a few of the alloys in which extra phases occurred. When data from an alloy not annealed with the standard procedure is reported the heat treatment used will be outlined.

The spin-echo spectra were taken with a variable-frequency spectrometer at about 1.3 K. A measurement of echo amplitude when suitably corrected provides a measure of the hyperfine-field distributions in the sample.[6] For the composition ranges presented in this paper all samples were ferromagnetic at 1.3 K.

III. Fe_3Si CRYSTAL AND MAGNETIC STRUCTURES

Fe_3Si is a crystallographically well-ordered ferromagnet. Its crystal structure, the face-centered-cubic DO_3 type, is shown in Fig. 1. This structure forms for alloys with compositions between about 10 and 26.5 at.% Si and has four sites A, B, C, and D with the specific neighbor configurations summarized in Table I. The notation Fe(B), Fe(A,C), and Fe(D) will be used to indicate Fe atoms in the B site, Fe atoms in either the A or C site, and Si atoms in the D site, respectively.

The Fe atoms on the two different sites B and A,C are chemically and magnetically different. Fe(A,C) has four Fe(B) and four Si(D) first neighbors (1NN), and a magnetic moment of $1.35\mu_B$.[7-9] The Fe(B) site has eight Fe(A,C) 1NN and a magnetic moment of $2.2\mu_B$.

In binary Fe-rich nonstoichiometric alloys the extra Fe replaces Si in the D sites producing Fe(A,C) sites

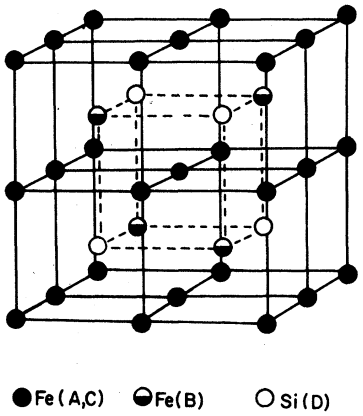

FIG. 1. Unit cell of Fe_3Si. The sites are labeled A, B, C, and D. The A and C sites are equivalent and are occupied by Fe atoms, the B site is occupied by Fe and the D site by Si.

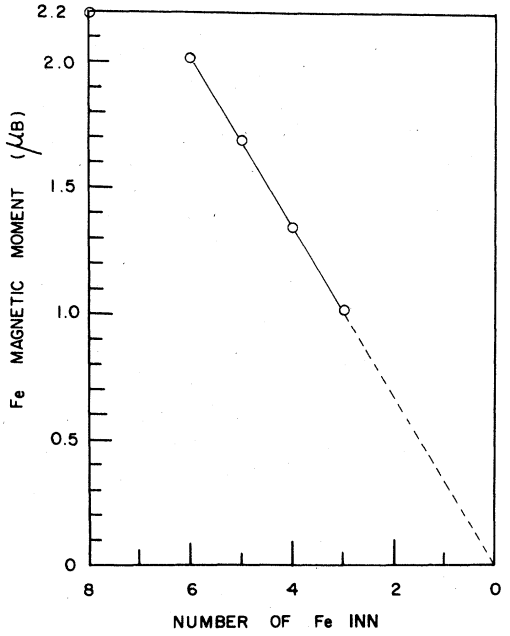

FIG. 2. Magnetic moment at the Fe(A,C) sites (in μ_B) vs the number of Fe 1NN for the binary Fe-Si system. The moment for eight Fe 1NN is $2.2\mu_B$. The solid line and closed symbols are taken by scaling the Fe moments with the corresponding hyperfine fields and the dashed line is a linear extrapolation.

with not only four but also five, six, and seven Fe(B) 1NN. In Si-rich nonstoichiometric alloys the extra Si replaces Fe in the B sites producing Fe(A,C) sites with three and two Fe(B) 1NN. Analogous changes are found in more-distant-neighbor configurations. Table I will be helpful in determining the effects of both nonstoichiometry and impurity substitution on various neighbor shells and for understanding the results on both binary and pseudobinary systems.

The magnetizations of the nonstoichiometric Fe_3Si alloys can be calculated by summing the atomic moments of its constituents. The pattern of Fe or Si substitution is assumed to be as described above and Fe atoms are assumed to have moments which depend only on the number of Fe atoms in their 1NN shell. Since nonstoichiometry involves extra Fe or Si on B sites, all Fe(B) keep a $2.2\mu_B$ moment while Fe(A,C) atoms have a variety of moments, derived from NMR and Mössbauer data, as described in Fig. 2.

In the pseudobinary substitutions of Mn and V in Fe_3Si the substituted atoms enter B sites. The magnetizations of these alloys are calculated by the

TABLE I. Near-neighbor configurations in the Fe_3Si system.

No. of shell	1	2	3	4	5	6	7	8
Neighbor distance in lattice parameters	0.43	0.5	0.705	0.83	0.86	1	1.08	1.11
A,C	4B 4D	6A,C	12A,C	12B 12D	8A,C	6A,C	12B 12D	24A,C
B	8A,C	6D	12B	24A,C	8D	6B	24A,C	24D
D	8A,C	6B	12D	24A,C	8B	6D	24A,C	24B

method described above with the additional requirements that Mn and V have moments of ~ 2.2 and $\sim 0\mu_B$, respectively, and like Si do not contribute to the Fe(A,C) moments. Fe(A,C) moments depend only on the numbers of their Fe first neighbors.[5]

IV. NMR SPECTRA OF $Fe_{3+x}Si_{1-x}$ ALLOYS

In Fig. 3 we show previously published spectra important for the understanding of the new NMR results for alloys containing substitutional impurities. Comparison of the spectra of these alloys with those of pseudobinary alloys based on the Fe_3Si matrix will lead to many of the conclusions reached in this investigation. Through NMR (Refs. 10 and 11) and Mössbauer-effect[12] studies the lines at about 46.59, 31.48, and 30.05 MHz in the Fe_3Si spectrum [Fig. 3(a)] have been identified as the resonances of Fe(B), Si(D), and Fe(A,C), respectively. (For consistency in this paper, the notation used to represent alloy concentrations and crystal sites has been changed from that used in many of the references.) The widths of these three lines are less than 100 kHz (which is less than the width of the lines drawn in the figure).

In the spectra of the two nonstoichiometric alloys [Figs. 3(b) and 3(c)] shifts due to first-neighbor interactions are clearly seen in the Fe(A,C) spectra.

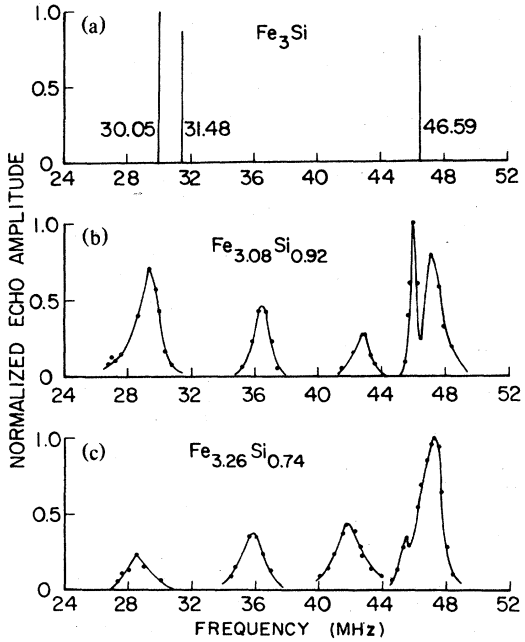

FIG. 3. (a)–(c) Spin-echo spectra, plots of normalized echo amplitude vs frequency of $Fe_{3+x}Si_{1-x}$ alloys with $x = 0$, 0.08, 0.26 at 1.3 K.

The extra Fe in these alloys replaces Si on D sites thus producing Fe(A,C) sites with not only four Fe and four Si but also five Fe and three Si and six Fe and two Si, in the first-near-neighbor shells. The lines at 29.9, 37.0, and 42.7 MHz seen in the spectra of $Fe_{3.08}Si_{0.92}$ and $Fe_{3.26}Si_{0.74}$ are from Fe atoms with these 1NN configurations.

The relative intensities of the Fe(A,C) lines and the concentration dependence of these relative intensities is consistent with the excess Fe entering the D sites randomly.

The shift for one extra Fe 1NN is 24% of the unperturbed Fe(A,C) frequency while that for two extra Fe 1NN is 43%.

The Fe(B) lines at 46.3 MHz have a satellite at about 47.2 MHz in the nonstoichiometric alloys. These satellites which are due to Fe in the Si site, a 2NN to Fe(B),[11] are shifted 1.9% of the frequency of the main line.

V. SUBSTITUTIONAL IMPURITIES

The spectra of the solute atoms themselves provide the clearest indications of the site occupied by that impurity in Fe_3Si, and for the most part we will concentrate the discussion upon them.

A. 3d impurities

1. A,C site substitution

a. Co. As mentioned earlier, atoms to the right of Fe in the periodic table show a strong preference for the Fe(A,C) site. Co is the clearest experimental illustration of an atom entering this site because of the intensity of the Co resonance and the separation of the Co resonance from the Fe and Si resonances. The behavior of the Co resonance in Fe-rich nonstoichiometric alloys provided the first evidence that a transition-metal ion substituted for Fe in Fe_3Si, had entered only the A,C site.[1]

In Fig. 4(a) the Co spectrum for a $Fe_{2.96}Co_{0.04}Si$ alloy is plotted. Note that there is only one symmetric line at about 194.6 MHz strongly suggesting that the Co has entered only one of the inequivalent Fe sites.

In Figs. 4(b) and 4(c) the Co and Fe spectra from a $Fe_{3.07}Co_{0.08}Si_{0.85}$ alloy are shown. The structure of the Co and Fe(A,C) spectra are remarkably similar. The relative intensities of both the Fe lines at 29.8, 36.4, and 42.5 MHz and the Co lines at 195, 230, 262, and 295 MHz are consistent with a random distribution of the excess Fe on Si sites and a random distribution of the Co on A,C sites.

The shifts in the frequency of the Fe(A,C) resonance due to one and two extra Fe 1NN are 22 and 43% of the principle Fe line, respectively. The com-

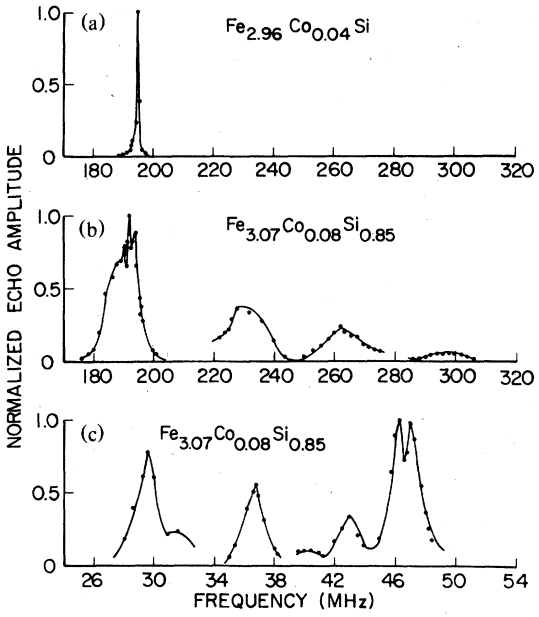

FIG. 4. Spin-echo spectra of Co in $Fe_{2.96}Co_{0.04}Si$ (a), $Fe_{3.07}Co_{0.08}Si_{0.85}$ (b), and Fe in $Fe_{3.07}Co_{0.08}Si_{0.85}$ (c), at 1.3 K.

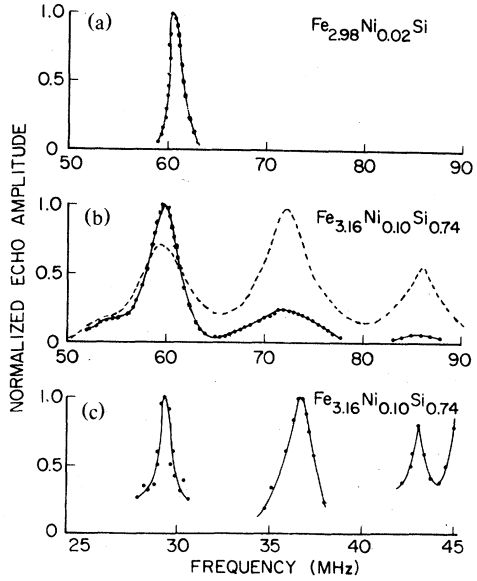

FIG. 5. Spin-echo spectra of ^{61}Ni in $Fe_{2.98}Ni_{0.02}Si$ (a), $Fe_{3.16}Ni_{0.10}Si_{0.74}$ (b), and Fe(A,C) in $Fe_{3.16}Ni_{0.10}Si_{0.74}$ (c), at 1.3 K.

parable shifts of the Co line, for the first three extra Fe 1NN, are 18, 34, and 51%.

The Fe and Si spectrum of $Fe_{3.07}Co_{0.08}Si_{0.85}$ shown in Fig. 4(c) is similar to that of the nonstoichiometric binary Fe_3Si alloys. See Figs. 2(b) and 3(c). Thus this line at 31.5 MHz is due to Si(D) and the lines at about 46.3 and 47 MHz are due to Fe(B) with eight Fe(A,C) 1NN. These Fe(B) atoms have six Si(D) or five Si(D) and one Fe 2NN, respectively.

The regularity in the observed cobalt spectra and the absence of a line that could be related to cobalt substitutions in the B site strongly argue that cobalt atoms select only A,C sites. This conclusion was firmly supported by subsequent neutron experiments on the same samples used in these experiments[2] as well as by a Mössbauer study of an $Fe_{3-x}Co_xSi$ alloy.[13]

b. Ni. An enriched ^{61}Ni isotope was used to prepare the samples used in these experiments. Spectra of ^{61}Ni in $Fe_{2.98}Ni_{0.02}Si$, and $Fe_{3.16}Ni_{0.10}Si_{0.74}$ are shown in Figs. 5(a) and 5(b), respectively. The relative positions of the principle lines and satellites are similar to those just described in the Co spectra and the lines have a similar explanation. In the stoichiometric alloy, Fig. 5(a), there is a single line at about 60.6 MHz, corresponding to an internal field of 159.99 kG. No other Ni resonance is observed indicating that Ni had entered only one of the Fe sites. In $Fe_{3.16}Ni_{0.10}Si_{0.74}$, a nonstoichiometric alloy, the main line is found at 59.7 MHz with clearly resolved satellites at 73.0 and 85.0 MHz. See Fig. 5(b). These lines because of their similarity to the Fe(A,C) spectrum are assigned to Ni atoms on A,C sites with four Fe and four Si, five Fe and three Si and six Fe and two Si 1NN, respectively. The shift due to one extra Fe 1NN is thus 19% of the frequency of the main line. The shift for two extra Fe neighbors is 42% of that frequency.

The intensities of the satellites relative to the main lines are, however, much smaller than those required for a random distribution of Ni on the A,C sites. The actual spectrum should be compared with the dashed line, which represents a hypothetical spectrum calculated using the assumptions: that Ni is randomly distributed over the A,C sites, that the intensity of the lines is proportional to the number of nuclei on each site, and that the lines are appropriately broadened. Results from nonstoichiometric alloys differing in composition are comparable. Clearly Ni shows a preference for those A,C sites with four Fe(B) and four Si(D) 1NN over those with a greater number of Fe 1NN.

Fig. 5(c) is the spectrum of the Fe and Si lines in the $Fe_{3.26}Ni_{0.10}Si_{0.74}$ alloy.

c. Cu. A number of attempts were made to prepare alloys with Cu substitutions. Unannealed samples were used since on annealing Cu separates from the Fe_3Si matrix. The x-ray data of one sample, $Fe_{2.96}Cu_{0.04}Si$, appeared to indicate a single phase. In this sample no resonance which could be attributed to Cu was observed.

2. *B* site substitution

a. Mn. The 3*d* elements that enter the *B* sites in Fe_3Si are to the left of Fe in the periodic table.[1] The NMR data over a wide range of Mn concentrations provides evidence that Mn prefers strongly the *B* sites.[4] In Figs. 6(a) and 6(b) the Mn(*B*) and Fe(*B*) spectra of a typical alloy, $Fe_{2.92}Mn_{0.08}Si$, are shown. The principle line of the Mn resonance is at about 273 MHz (258.8 kG). This line and its satellites at about 267.8 and 262 MHz are the only lines in the Mn spectrum, indicating that Mn enters only one Fe site. The similarity between the Mn and the Fe(*B*) spectra strongly suggest that Mn occupies *B* sites. Further, the relative intensities of the lines in both the Fe(*B*) and the Mn spectra are approximately proportional to the distribution of *B* sites with different numbers of Mn 3NN which would be produced by a random distribution of Mn on *B* sites. The shift in the Mn resonance for each Mn 3NN is −5.2 MHz, or 1.9% of the frequency of the principle line. Each Mn 3NN shifts the Fe(*B*) line 1.2 MHz or 2.5%.

In spectra for the nonstoichiometric alloy, $Fe_{3.03}Mn_{0.052}Si_{0.92}$, Fig. 6(c) the Mn lines at 273.2 and 267.6 have clearly resolved satellites at 277 and 270.6 MHz, respectively. The relative intensities of these satellites to those of the main lines are proportional to the numbers of *B* sites which have five Si and one Fe 2NN to those with six Si 2NN due to Fe in *D* sites. This shift is about 3.6 MHz, 1.3% of the main-line frequency. In the same alloy the shift of the Fe(*B*) line due to 2NN is 0.8 MHz, or 1.9%.

Note that a similar satellite is found in the spectra of Fe(*B*) in nonstoichiometric Fe_3Si alloys. [See Figs. 3(b) and 3(c).]

Thus the shifts at *B* site atoms produced by 2NN and especially 3NN clearly demonstrate that Mn enters the *B* sites.

Further studies of $Fe_{3-x}Mn_xSi$ for higher concentrations supports the strong preference for the *B* site substitution up to about $x=0.74$.[4] Independent neutron studies by Yoon and Booth[14] have reached a similar conclusion for the Mn site preference.

b. Cr. Neutron scattering has shown that Cr enters the *B* sites in Fe_3Si.[2] The Fe(*B*) sites NMR data support this conclusion. Figure 7(a) shows the Fe(*B*) spectrum of a $Fe_{2.92}Cr_{0.08}Si$ alloy. The relative intensities of the lines, split about 1 MHz or 2.1%, are consistent with the numbers of *B* sites with different numbers of Cr 3NN due to a random distribution of Cr on the *B* sites.

The Cr resonance was not observed. The internal field of Cr in Fe has been reported at 10(4) kG (2.4 MHz).[15] Using this information and for reasons to be explained in the discussion a predicted resonant frequency for Cr in Fe_3Si of about 1.3 MHz is obtained. This frequency is below the effective range of our spectrometer. An extensive search for the Cr resonance between 10 and 100 MHz on samples made with an enriched ^{53}Cr isotope did not produce any signal attributable to Cr. This supports the conjecture that the Cr frequency is lower than 10 MHz.

c. V. The spectra of the $Fe_{3-x}V_xSi$ alloy, except

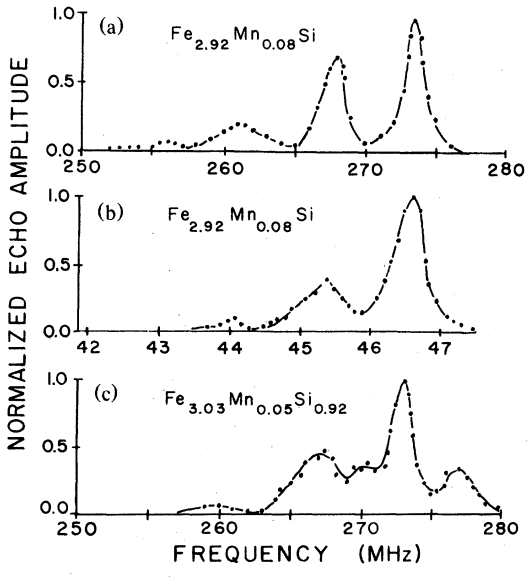

FIG. 6. Spin-echo spectra at 1.3 K of Mn in $Fe_{2.92}Mn_{0.08}Si$ (a), Fe in the same alloy (b), and Mn in nonstoichiometric $Fe_{3.03}Mn_{0.05}Si_{0.92}$ (c).

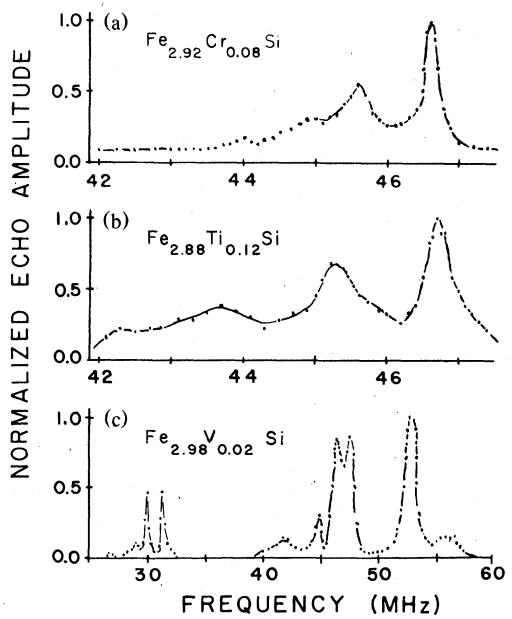

FIG. 7. Spin-echo spectra of Fe(*B*) in $Fe_{2.92}Cr_{0.08}Si$ (a), of Fe(*B*) in $Fe_{2.88}Ti_{0.12}Si$ (b), and of Fe(*B*), V(*B*), Fe(*A*,*C*), and Si(*D*) in $Fe_{2.98}V_{0.02}Si$ (c).

for the frequency of the V resonance (53.0 MHz, 47.7 kG) are almost identical to those of a Mn alloy of equal x, and thus would merit the same interpretation. V clearly enters the B sites. The splitting of the V spectrum due to one 3NN V atom is 5.4 MHz, 10.2%. This shift is about 4.8 kG and is almost identical to that produced in the Mn spectrum by a single Mn 3NN. The spectrum of a $Fe_{2.98}V_{0.02}Si$ alloy is shown in Fig. 7(c). Note that the V(B) and Fe(B) spectra overlap. For further details see Ref. 5.

d. Ti. The fact that Ti in Fe_3Si enters the B site was determined by neutron scattering.[2] The NMR data support this conclusion. A level of disorder higher than that found in Mn, Cr, and V alloys is characteristic of the Ti series. Figure 7(b) is a plot of the Fe(B) spectrum from a $Fe_{2.88}Ti_{0.12}Si$ alloy. The shift in the Fe(B) line due to one extra Ti 3NN is about 1.7 MHz or 3.6%, significantly larger than the shifts due to Mn, Cr, and V. The lines from Fe nuclei on sites with zero and one Ti 3NN are anomously weak. Possibly, this is due to a clustering of Ti in these samples.

Ti has two NMR isotopes with essentially equal gyromagnetic ratios, 2.400 and 2.401 kHz/10 kG with a combined natural abundance of 13.26%. The Ti resonance was not observed from 10 to 200 MHz. Since the Ti resonance has not been observed in Fe no prediction of its resonant frequency in Fe_3Si was attempted.

3. Discussion of site hyperfine-field shifts

a. B site field shifts. A model which correlates x-ray, magnetization, neutron-diffraction, and spin-echo NMR results in the $Fe_{3-x}Mn_xSi$ and $Fe_{3-x}V_xSi$ systems over a large range of concentrations is now discussed. The fact that this model considers only contributions to the hyperfine field from spin polarizations due to the moment of the atom itself and the moments of its 1NN emphasizes the local character of interactions in these alloys. More-distant neighbors affect the field indirectly by altering the moments of the 1NN. This presentation is a brief summary of already published results. For a complete discussion see Ref. 5.

The internal field at an atom on B site can be written

$$H_{\rm int}(B) = [H_{\rm cp}(B) + H_s(B)] + H_{sp}(B) \qquad (1)$$

where $H_{\rm cp}$ and H_s are the core polarization and conduction-electron polarization (CEP) contributions due to the atom itself, and H_{sp} the overall CEP contributions from the 1NN atoms.

The replacement of an Fe(B) atom with a V or Mn atom introduces disturbances into the 3NN shells of resonant Fe(B), V(B), or Mn(B) nuclei (see Table I). At low concentrations these disturbances produce resolvable satellites in the NMR spectra as seen in Figs. 6(a)–6(c), and 7(c). The satellite shifts are proportional to the number of atoms substituted in the third-neighbor shells. Figure 8 is a plot of the internal fields of satellites in Fe(B), Mn(B), and V(B) spectra versus calculated values of $\bar{\mu}(A,C)_{\rm 1NN}$, the average moment of their eight Fe(A,C) first near neighbors. [$\bar{\mu}(A,C)_{\rm 1NN}$ is calculated by inspecting the first-neighbor shells of each of the eight Fe(A,C) 1NN of a B site for Fe atoms and assigning moments according to the model described in Sec. III which requires that the moments of Fe(A,C) atoms depend on only the number of their first-neighbor Fe atoms.] The field shifts of the satellites in Fig. 8 are clearly linearly dependent on the average 1NN moment. Thus the substitution of Mn and V atoms in the 3NN shell of a B site nucleus reduces the magnetic moments of the substituted atom's Fe(A,C) 1NN and these 1NN in turn affect the hyperfine fields of their B site first neighbors, presumably via 4s-spin polarization.

The contributions from the atom itself to the internal field at the resonant B nucleus is [$H_{\rm cp}(B)$

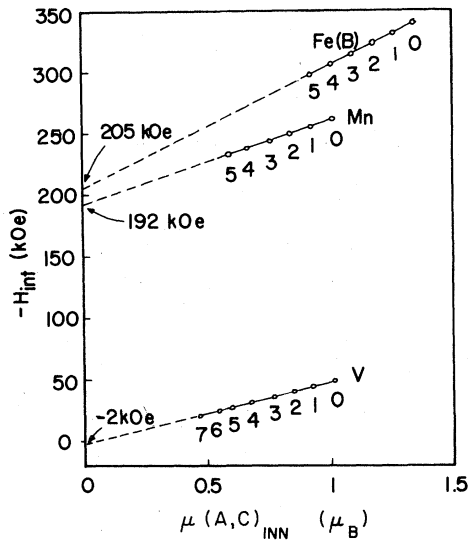

FIG. 8. $H_{\rm int}$ for Fe(B), V(B), and Mn(B) corresponding to different satellites in $Fe_{3-x}T_xSi$ (T = V, Mn) vs average magnetic moment in the 1NN shell. The numbers 0, 1, 2, . . . indicate the fields corresponding to 0, 1, 2, . . . substituted atoms in the 2NN shell. For Fe(B) the first two fields (0,1) have identical positions for both Mn and V substitutions. Fields 3, 4, and 5 could be observed only in $Fe_{3-x}Mn_xSi$, because in V alloys the V spectrum overlaps the Fe spectrum at concentrations $x > 0.04$. From the slope of the $H_{\rm int}(\mu)$ lines one can derive the value of the polarization np due to the 1NN moment and the intercept with the ordinate axis gives the on-site hyperfine fields ($H_{\rm cp} + H_s$).

$+H_s(B)]$ and this contribution can be separated by an extrapolation of $H_{int}(B)$ vs $\bar{\mu}(A,C)_{1NN}$ to 0 (Figure 8.) The extrapolated values for H_{int} found for Fe, Mn, and V are −205, −192, and +2 kOe, respectively. Using the measured-site moment for Fe(B), $2.2\mu_B$, and the extrapolated value of the internal field at $\bar{\mu}(A,C)_{1NN}=0$, −205 kOe, a self-polarization of −93.18 kOe/μ_B is obtained for Fe(B). Assuming the same self-polarization for Mn and V ions and using their extrapolated fields, −192 and +2 kOe, local moments of $2.06\mu_B$ for Mn and $-0.02\mu_B$ for V are obtained. These calculated moments agree with those needed to explain magnetization and neutron-diffraction data. See Sec. III.

$H_{sp}(B)$, the hyperfine-field contribution from neighboring atoms can be related directly to the 4s-spin polarization in the neighborhood of Fe(A,C) atoms by the formula

$$H_{sp}(B)=a_{4s}(B)\bar{\mu}(A,C)_{1NN}np \ , \qquad (2)$$

where $a_{4s}(B)$ is the 4s hyperfine coupling constant in units of Oe/μ_B, n is the number of 4s electrons involved in the hyperfine coupling, and p the intensity of coupling between the 4s electrons and the Fe(A,C) first-near-neighbor moments. In the analysis described, there is insufficient data to find both n and p and, thus, their product must be considered.

By using the hyperfine coupling parameters $a_{4s}(B)$ as calculated by Campbell[16] values for the product np have been derived. (See Table II, column 5.) The results show that the spin polarizations produced by the exchange coupling between the 4s spins in the vicinity of the resonant nucleus and the Fe(A,C) magnetic moments in the 1NN shell are essentially the same for V, Mn, and Fe. The product np for these three cases should be the same if satellite structure in the spectra is due to Fe(A,C) moments polarizing 4s conduction electrons.

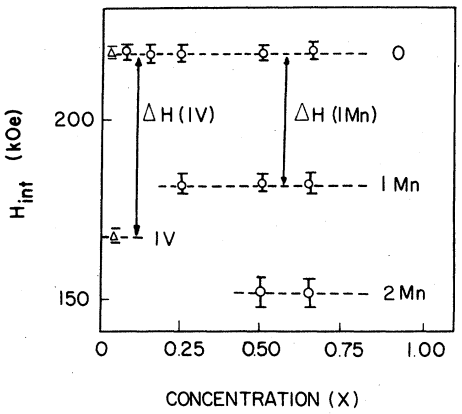

FIG. 9. H_{int} Fe(A,C) corresponding to different satellites of Fe(A,C) in $Fe_{3-x}Mn_xSi$ (○) and $Fe_{3-x}V_xSi$ (Δ) vs concentration. This figure is taken from Ref. 5.

b. A,C site field shifts. Equations similar to (1) and (2) can be used to obtain the on-site and transferred contributions to Fe(A,C) hyperfine fields. The substitution of Mn or V in Fe_3Si produces satellites on the low-frequency sides of the Fe(A,C) spectra. See Fig. 9.

$[H_{cp}(A,C)+H_s(A,C)]$ is obtained by assuming that the on-site contribution to the internal fields of Fe(A,C) atoms are proportional to their magnetic moment at −93.18 kOe/μ_B, the same self-polarization as Fe(B). Using this value and the measured $H_{int}(A,C)$, in Eq. (1), $H_{sp}(A,C)$ can be found for several different 1NN configurations [e.g., four Si and four (Fe+Mn) or four Si and four (Fe+V)]. Equation (2) then yields average values of the CEP, $\overline{np}$, of $-46(3)\times10^{-3}/\mu_B$ for Mn and $-49(2)\times10^{-3}/$

TABLE II. Hyperfine fields in $Fe_{3-x}V_xSi$ and $Fe_{3-x}Mn_xSi$ alloys. Summary of the contributions to the measured internal field for Fe, V, and Mn in various sites calculated according to the model (Ref. 5). The values of the magnetic moments are calculated from the internal field data by taking $\mu(\text{Fe}(B))=2.2\mu_B$. The values for $a_{4s}(Z)$ are taken from Ref. 16.

Nucleus	1NN configuration	$a_{4s}(Z)$	$H_{cp}+H_s$ (kOe)	np (10^{-3})	Calc. (μ_B)
V(B)	8 Fe(A,C)	1.11	+2	−44	−0.02
Mn(B)	8 Fe(A,C)	1.54	−192	−44	2.06
Fe(B)	8 Fe(A,C)	1.78	−205	−56	2.2
Fe(A,C)	4 (Fe+Mn) 4 Si	1.78		−46(3)	
Fe(A,C)	4 (Fe+V) 4 Si	1.78		−49(2)	

μ_B for V substitutions. These values of $\overline{np}$ are essentially equal to those found for Fe, Mn, and V atoms on B sites. This result further confirms the fact that the local-spin polarization produced by the exchange coupling between the $3d$ magnetic moments and the $4s$ spins is proportional to the magnitude of the 1NN magnetic moments. The extensive agreement of the model with the experiment supports the original assumption that the Fe(A,C) moments depend on only the number of Fe 1NN. Since the substitution of Si, Mn, or V for Fe(B) reduces the Fe(A,C) moment by nearly equal amounts, it is clear that this moment perturbation depends most strongly on the number of Fe 1NN to Fe(A,C) rather than on the individual moments of the neighboring substituted Si, V, or Mn.

These results allow one to separate in an unambiguous way the on-site and neighbor contributions to the hyperfine field at the transition metal in the $Fe_{3-x}T_xSi$ systems. The model provides the first direct evidence that the interactions in Fe_3Si and its alloys with V and Mn may be short range and the interactions with more-distant neighbors indirect. Specifically, the hyperfine-field contributions from the polarization of $4s$ electrons are due to interactions with moments at the 1NN shell, and more-distant neighbors contribute to CEP by perturbing the 1NN shell moments of a given B site. Except for these indirect effects, Fe(A,C) seems to screen B atoms from any direct interaction with a more-distant neighbor either magnetically or chemically.

As seen in Fig. 5, the Fe(B) spectra of Cr and Ti are very similar to that of Mn in that they show structure which by analogy we associate with 3NN effects, a conclusion supported by neutron data which directly establishes B site selection for both Ti and Cr. This leads us to believe that the model just discussed applies to these alloys as well. However the absence of solute spectra makes a rigorous application of the model difficult.

These results could provide a new theoretical direction for the calculations of magnetic moments and internal fields at the $3d$ elements. As shown before, the NMR satellite structure for both the host (Fe) and the V and Mn impurities in dilute alloys bears a close resemblance to the spectra of the same elements in Fe_3Si. This striking feature can be considered in the light of recent experimental results of Khoi *et al.*[17] which show that certain impurities in an Fe host prefer certain neighbors. With this additional knowledge it should be possible to examine the internal-field distributions in dilute alloys with a fresh approach. The conclusion that an Fe atom carries a moment of $2.2\mu_B$ as long as it is surrounded in the 1NN shell by eight Fe irrespective of their moments, is consistent with the work of Parthasarathi and Beck.[18] These authors have suggested, from an analysis of their magnetization data on Fe alloys, that an Fe atom, surrounded by eight Fe atoms with no moment, still carries a moment of $2.2\mu_B$.

B. 4*d* impurities

1. Fe(A,C) substitution

The $4d$ metals Ru, Rh, and Pd enter the A,C sites in Fe_3Si. In nonstoichiometric alloys they do so nonrandomly, preferring to replace Fe(A,C) on those sites with four Fe(B) and four Si(D) neighbors. These spectra in various Fe_3Si matrices are very similar to those of Ni in the same matrix and require similar explanations.

a. Ru. In Fig. 10(a) the Ru spectrum from a $Fe_{2.96}Ru_{0.04}Si$ alloy clearly shows lines from the ^{101}Ru and ^{103}Ru isotopes at 53.8 and 60.2 MHz, respectively, an internal field of about 283 kG. The partially resolved satellites at 56.5 and 63.0 MHz are probably owing to a single Ru 3NN. Figure 10(b) shows the spectrum of a $Fe_{3.18}Ru_{0.08}Si_{0.74}$ alloy. The lines of low intensity at about 68 and 74 MHz are due to Ru in a a site with five Fe and three Si 1NN. For comparison with this data, a spectrum calculated assuming a random distribution of Ru on all Fe(A,C) sites, is shown with a dashed line. Thus like Ni, Ru shows a configurational preference for Fe(A,C) sites with four Fe and four Si 1NN in nonstoichiometric compositions.

b. Rh. Figure 11(a) shows the spin-echo spectrum for Fe, Si, and Rh in a $Fe_{2.96}Rh_{0.04}Si$ alloy. The Rh line is at 39.4 MHz (294 kG). In Fig. 11(b) the spectrum of a $Fe_{3.10}Rh_{0.16}Si_{0.74}$ is plotted. In this alloy a large amount of Rh has been used so that the contributions of Fe and Si to the total spectrum will be small. The lines at about 38.1 and 47 MHz are due to Rh with four Fe and four Si and five Fe and three Si 1NN, respectively. If Rh were distributed random-

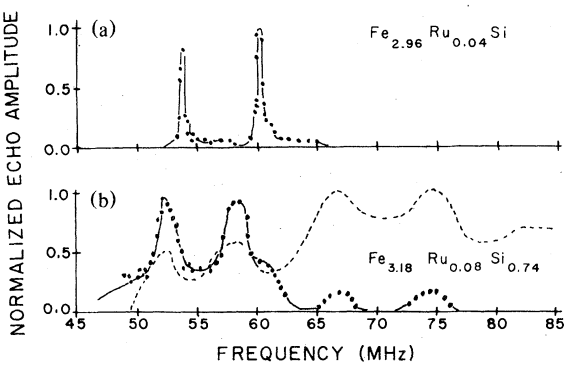

FIG. 10. Spin-echo spectra of ^{101}Ru and ^{103}Ru in $Fe_{2.96}Ru_{0.04}Si$ (a), and in $Fe_{3.18}Ru_{0.08}Si_{0.74}$ (b); the dashed line corresponds to a calculated spectrum assuming a random distribution of Ru on A,C sites.

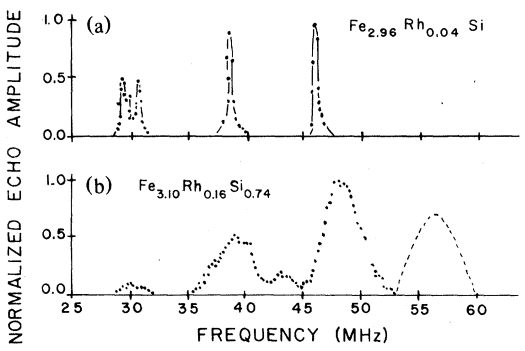

FIG. 11. Spin-echo spectra of Rh in $Fe_{2.96}Rh_{0.04}Si$ (a), and in $Fe_{3.10}Rh_{0.16}Si_{0.746}$ (b), the dashed line corresponds to a line which should appear assuming a random distribution of Rh on A,C sites.

ly over the A,C sites a line at about 56 MHz owing to Rh with six Fe and two Si neighbors should be clearly seen. This undetected line is shown by dashes in Fig. 11(b). The measured spectrum indicates that Rh enters Fe(A,C) sites with four Fe and four Si and five Fe and three Si 1NN almost randomly but avoids the sites with six Fe and two Si 1NN.

c. Pd. The Pd-substituted Fe_3Si alloys exhibit special metallurgical problems. X-ray diffraction showed a Pd_2Si second phase in all samples. Since Pd_2Si is not ferromagnetic it does not contribute to the NMR spectra presented in this paper. The Pd NMR signals reported here are strongly dependent on heat treatment. The signals could be seen in as crushed powders or powders quenched from above 600 °C. When one of the Pd alloys was annealed and then furnace cooled from 600 °C the signal was lost, probably indicating a precipitation of the Pd_2Si phase at these temperatures. Thus only those analyses of the Pd spectra can be made for which an exact knowledge of the degree of stoichiometry or of the exact Pd concentration is not a factor.

Figure 12(a) shows the Pd spectrum at 58.5 MHz (3.36 kG) in a $Fe_{2.85}Pd_{0.15}Si$ alloy. In Fig. 12(b) two Pd lines at about 53 and 71 MHz are shown in a nonstoichiometric alloy $Fe_{2.84}Pd_{0.24}Si_{0.92}$ alloy. The dashed line spectrum indicates the intensity expected at 71 MHz if Pd had entered the Fe(A,C) sites randomly.

A conclusion that Pd enters the Fe(A,C) site nonrandomly can be made in spite of the presence of the Pd_2Si phase. The formation of this phase would further delete the Si content of the Fe_3Si-type alloy and leave it further from stoichiometry thus enhancing the number of AC sites with extra Fe 1NN. However, the Pd spectra of the nonstoichiometric alloys could be explained only by the occurrence of a matrix composition significantly closer to stoichiometry.

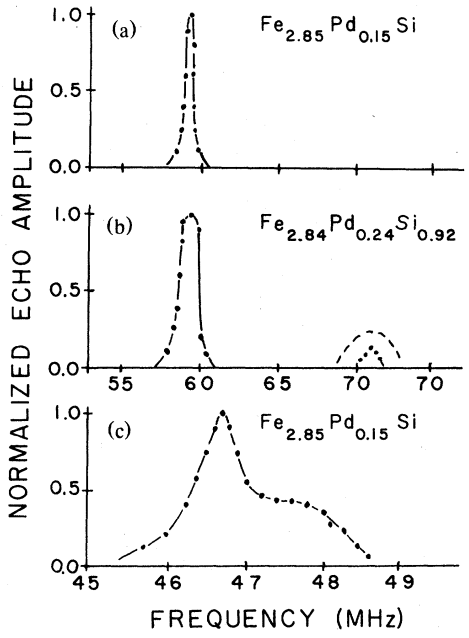

FIG. 12. Spin-echo spectra of Pd in $Fe_{2.85}Pd_{0.15}Si$ (a), and in $Pd_{2.84}Pd_{0.24}Si_{0.92}$ (b) the dashed line corresponds to a calculated spectrum assuming a random distribution of Pd on A,C sites, and of Fe in $Fe_{2.85}Pd_{0.15}Si$(c).

d. Ag. A very limited number of attempts following standard procedures, were made to prepare substitutional alloys of Ag in Fe_3Si. X-ray spectra of these alloys showed two phases Ag and Fe_3Si.

2. *Mo and Nb alloys*

a. Mo. Mo samples showed a second phase, (Fe_2Mo), with the $C14$-type hexagonal Laves structure at all concentrations tested. In the NMR spectrum of one as crushed alloy made with enriched ^{95}Mo, we observed the Fe_3Si spectrum accompanied by an extra line. A large quantity of systematic data will be necessary to assign this resonance to a definite site in one of the phases.

b. Nb. Nb substituted samples also showed a second phase of the $C14$ (Fe_2Nb) structure in all of the alloys except for a very dilute sample, $Fe_{2.975}Nb_{0.025}Si$. The slight difference in the lattice parameter from Fe_3Si could be due either to Nb entering Fe_3Si matrix or to a slightly Si-rich sample due to the loss of Nb during arc melting. No Nb resonance was observed in this sample over a wide frequency range around the value deduced from the Nb field in Fe metal.

C. 5*d* substitutions

1. A,C site substitution

a. Os. Os, the 5*d* element under Fe in the periodic table, enters the *A,C* site and does so randomly in nonstoichiometric alloys. The Os resonance occurs at 241 MHz (1130 kG) in the spectrum for $Fe_{2.85}Os_{0.15}Si$ shown in Fig. 13(a). The satellite due to the addition of an extra Fe atom in the 1NN shell is shifted 45 MHz to higher frequency in the spectrum of $Fe_{2.84}Os_{0.24}Si_{0.92}$. See Fig. 13(b). The intensity ratios this satellite to the main line appears to be consistent with a random distribution of Os in *A,C* sites with different numbers of Fe 1NN. It is observed that a number of partially resolved satellites occur on the low-frequency side of the principle Os line. Since these satellites are not visible in the spectrum of the stoichiometric alloy, Os in the 2NN and 3NN shells seems to be eliminated as an explanation and changes in the 4NN shell seems to be the most likely cause. See Table I.

b. Ir. Figure 14(a) is the spectrum of Ir in $Fe_{2.96}Ir_{0.04}Si$. Partially resolved lines corresponding to the isotopes ^{191}Ir and ^{193}Ir are seen at 64.8 and 70.2 MHz. As is the case for Ir in Fe these lines are split by a definite quadrupole interaction shown by the partially resolved satellites occurring at 63.0 and 66.6 MHz for ^{191}Ir and at 68.4 and 72.0 for ^{193}Ir. The frequency shift for these satellites is about ± 8 MHz in both cases and the 3:4:3 intensity ratio of satellites to main-line characteristic of nuclei with $\frac{3}{2}$ spin is verified for both isotopes. The ratio of the resonant frequencies of the main lines is 1.06 approximately the ratio of the gyromagnetic ratios. Also the ratio of the integrated intensities of the resonances is about 1.59

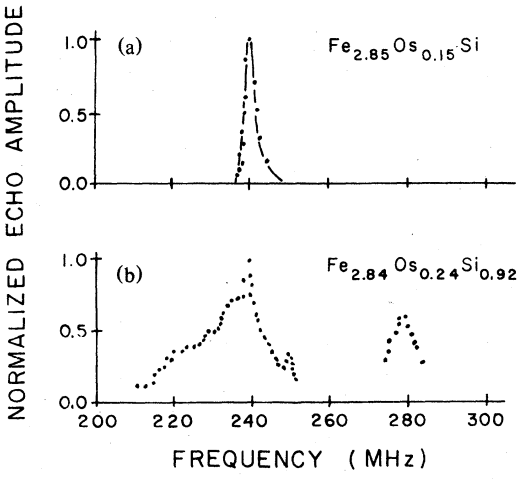

FIG. 13. Spin-echo spectra of Os in $Fe_{2.85}Os_{0.15}Si$ (a) and $Fe_{2.84}Os_{0.24}Si_{0.92}$ (b).

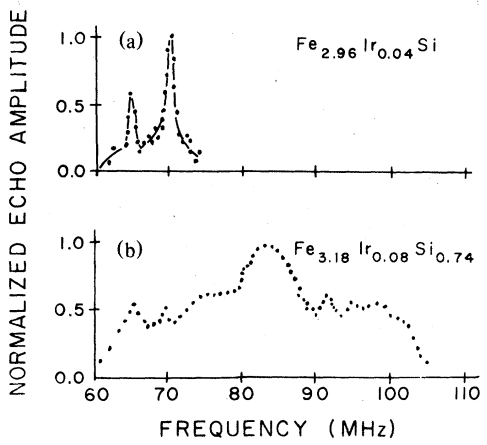

FIG. 14. Spin-echo spectra of ^{191}Ir and ^{193}Ir in $Fe_{2.96}Ir_{0.04}Si$ (a) and $Fe_{3.18}Ir_{0.08}Si_{0.74}$ (b).

consistent with the ratio of the natural abundances of the isotopes. The Ir spectrum of a $Fe_{3.18}Ir_{0.08}Si_{0.74}$ alloy is shown in Fig. 14(b). This is a complicated spectrum with at least 18 lines. A reasonable fit is obtained assuming a random distribution of Ir on *A,C* sites and a splitting of about 15 MHz for each extra Fe 1NN. In this and other spectra of the nonstoichiometric alloys a broadening and shift to lower frequency makes it likely but not certain that there is a shift in the spectrum due to changes in the Ir 4NN shell similar to that seen in Os alloys.

c. Pt. X-ray data on a limited number of $Fe_{3-x}Pt_xSi$ samples show a second phase. The Pt resonance in Fe is at about 1171 MHz leading to a predicted value for Pt in Fe_3Si of about 600 MHz, well above the effective range of our spectrometer.

d. Au. X-ray data indicate that $Fe_{3-x}Au_xSi$ alloys are composed of Fe_3Si and Au metal phases. However NMR intensity between 49 and 63 MHz in several very dilute alloys indicates that some small amount of Au has entered the Fe_3Si phase. The width of this spectrum is about two orders of magnitude broader than the lines observed for other dilute substitutions of elements which are easily soluble in Fe_3Si.

2. Re, W, and Ta alloys

a. Re. Re in Fe_3Si forms single-phase alloys at least up to concentrations of $x = 0.12$. The Re resonance has not been observed between 10 and 500 MHz. Since the ^{187}Re resonance in Fe is about 736 MHz we would expect its resonance in Fe_3Si at about 405 MHz.

The Fe and Si resonances in $Fe_{2.92}Re_{0.08}Si$ alloy Fig. 15(a) would be consistent with the entry of Re into

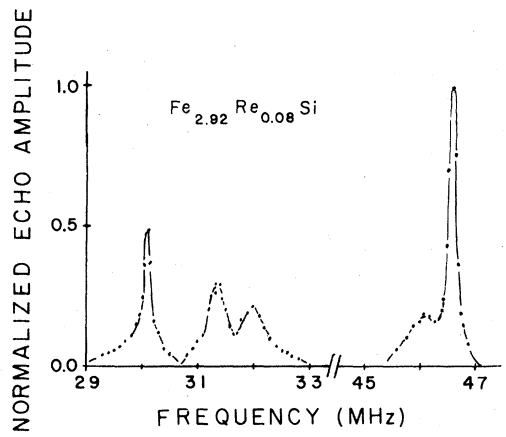

FIG. 15. Spin-echo spectrum of Re in a $Fe_{2.92}Re_{0.08}Si$ alloy.

the *B* site. However the line corresponding to sites with 0 Re and 12 Fe 3NN is larger than would be required by a random distribution. For a definite assignment of Re to *B* sites either data on the Re resonance or neutron scattering experiments would be necessary.

b. W. W substitutions in Fe_3Si precipitates the $C14$ phase Fe_2W at all concentrations.

c. Ta. X-ray data showed the $C14$ phase Fe_2Ta in many alloys but one of the Ta alloys, $Fe_{2.88}Ta_{0.12}Si$, was single phase. The Ta resonance was not found during an extensive search from 10 to 500 MHz. A rough prediction of the frequency of this resonance, based on the Ta resonance in Fe(333.9 MHz), is 184 MHz. The broadening of the Fe and Si lines and the presence of satellites indicated that Ta had entered the Fe_3Si matrix.

VI. DISCUSSION AND ANALYSIS OF SELECTIVE SITE OCCUPATION

Thus NMR measurements have clearly shown that transition metals at dilute concentrations enter one of the two inequivalent Fe sites. The 3*d* elements to the left of Fe in the periodic table Mn, Cr, V, and Ti replace Fe in the *B* site and those to the right replace Fe in the *A,C* site. The 4 and 5*d* elements to the left of Fe are for the most part insoluble in Fe_3Si.

A. Similarity with the Heusler alloys

The relationship between the position of a transition metal relative to Fe in the periodic table and the site it enters in Fe_3Si is apparent. Table III (a) shows portion of the periodic table, blocked off with solid lines, to indicate that atoms to the left of Fe enter

TABLE III. Periodic table showing that the site an impurity enters in Fe_3Si depends on its location in (a). A table showing the same for the Heusler alloys (b). Heavy lines are used to indicate elements that substitute in *B*, *A,C*, and *D* sites, dashed lines to show the metals to the left side that form the Fe_2T second phase and those to the right which do not form a single-phase material.

(a)

IIIB	IVB	VB	VIB	VIIB	VIIIB		IB	IIB	IIIA	IVA
B site					AC site				D site	
									Al	Si
	Ti	V	Cr	Mn	Fe	Co	Ni	Cu		
		Nb	Mo		Ru	Rh	Pd	Ag		Sn
		Ta	W	Re	Os	Ir	Pt	Au		

(b)

IIIB	IVB	VB	VIB	VIIB	VIIIB		IB	IIB	IIIA	IVA	VA	VIA
B site					AC site				D site			
									Al	Si	P	S
Sc	Ti	V	Cr	Mn	Fe	Co	Ni	Cu	Zn	Ga	Ge	As	Se
Y	Zr	Nb	Mo	Tc	Ru	Rh	Pd	Ag	Cd	In	Sn	Sb	Te
Zr	Hf	Ta	W	Re	Os	Ir	Pt	Au	Hg	Tl	Pb	Bi	Po

the *B* sites and those under Fe or to the right of Fe enter *A,C* sites. Re has been included among the *B* site occupiers although this identification is tentative. Fe is included among both the *B* and *A,C* occupiers. Also indicated with a solid line are Si, Al, and Sn the atoms known to enter the *D* sites. Those atoms to the left which precipitate Fe_2T as a second phase are enclosed with dashed line as are those atoms to the right which are either insoluble or precipitate a second phase.

The context of selective site occupation in Fe_3Si can be expanded by comparing the pseudobinary Fe_3Si alloys to the Heuslers, a large class of similar materials, of which Cu_2MnAl is the prototype. Indeed, this similarity may be emphasized by choosing to describe Fe_3Si by the $L2_1$ crystal structure. The formula $Fe(A,C)_2Fe(B)Si$ would then be used because of the different chemical and magnetic properties of the two Fe sites. With a few exceptions involving atoms like Li and Mg, the Heusler alloys are formed from a transition metal to the right of Fe in the periodic table in the Mn site (*B* site), one to the right of Fe in the Cu site (*A,C*) site, and a nontransition metal to the right of Fe in the table in the Al site (*D* site). See Tables III (a) and III (b). For Mn, V, and Co substitutions in Fe_3Si, where alloys over a

wide range of x are possible, Heusler-type alloys form at the concentrations: Fe_2MnSi, Fe_2VSi, and Co_2FeSi (Ref. 19) further emphasizing the similarity of Fe_3Si and the Heusler structures. For the above elements solubility studies have shown that Mn is soluble over the whole range of concentrations and Mn_3Si has the DO_3 crystal structure. V and Cr are soluble to about $x=1$ and V_3Si and Cr_3Si have $A15$-type crystal structures. Co is soluble to about $x=2$, the solubility of Ni is limited to about $x=1$ and Ti to about $x=0.75$. At least for $3d$ elements the amount of an element that can be dissolved in Fe_3Si decreases as the impurity is separated from Fe in the periodic table. As previously shown the limits of solubility in Fe_3Si for the $3d$ elements are clearly dependent on the concentration of the outer, $s+p+d$, electrons. The lower limit is 6.25 electrons per atom and the upper limit is 7.5 electrons.[20] For the $4d$ and $5d$ elements further studies are required for an accurate determination of solubility limits.

B. Atomic size and electronegativity

A standard method of estimating the solubility of elements in metals is from a Darken-Gurry plot.[21] In this plot the electronegativity and the metallic radii of the solutes are compared to those of the solvent. Good solubility generally occurs if these properties of the solute do not differ by more than 15% from those of the solvent. Although it is not possible to assign a metallic radius or electronegativity to the solvent Fe_3Si or to any of its sites a plot of the electronegativity versus metallic radii for the solutes can be useful in discussing the role of these parameters in site selection in Fe_3Si and the Heusler alloys. The Pauling radii for coordination number 8 are used. See Fig. 16.

From an analysis of the figure it seems apparent that electronegativity is an important factor in site selection. The electronegativities of those atoms entering the A,C sites are larger than those of the atoms entering the B sites. For the B site occupants the electronegativity varies from 1.5 to 1.8 and, if Fe is not considered the variation is only from 1.5 to 1.6. The electronegativity of the A,C site atoms varies from 1.8 to 2.4. The larger electronegativities of the A,C site atoms is consistent with a picture in which Fe(A,C) bonds covalently with Si(D). Such bonding has often been proposed to explain the different magnetic moments and internal fields at the Fe(B) and Fe(A,C) sites.[22]

The conclusion, reached on the basis of electronegativity, that the B site prefers atoms which can give electrons and the A,C site prefers atoms which can receive electrons is consistent with the band-structure model of Switendick.[23] It is possible with the data as they now exist to conclude that there is a

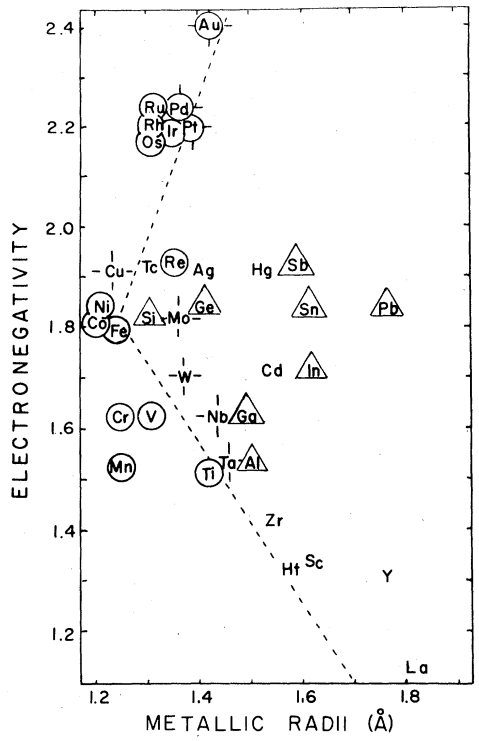

FIG. 16. Electronegativity plotted against metallic radii, for the elements in pseudobinary Fe_3Si and Heusler alloys. Each element is represented by its chemical symbol. Those entering the B and A,C sites in Heuslers are not further marked, the symbols of those found in Heusler D sites are enclosed in a triangle. A circle around a symbol indicates that the element enters a B or an A,C site in Fe_3Si and those elements which cause the formation of a second phase in Fe_3Si are marked with a cross. The dashed lines are intended to illustrate the approximate ranges of size and electronegativity of the atoms found in each site in Fe_3Si.

general relationship between electronegativity size and site selection as indicated in Fig. 16, but we cannot draw specific boundaries for these systematics. The charge transfer to Fe(A,C) sites would account for its reduced atomic moment.

This phenomenological conclusion derived from our experimental work is very similar to deductions from the band-structure calculations on Fe_3Si by Switendick,[23] as shown in Sec. VI C and the work of Jena and Geldart[24] on Heusler alloys.

On the other hand atomic size does not seem to be a determining factor in site selection since the ranges of size of atoms known to enter the Fe(B) and Fe(A,C) sites are approximately the same. The metallic radii of the A,C site impurities vary from 1.15 to 1.34 Å. These variations are 17 and 15%, respectively. From these considerations we cannot con-

clude whether atoms like Au, Ag, Hg, and Cd which are larger than 1.34 Å are prohibited by their size from entering A,C sites, and atoms like Zr, Hf, Sc, Y, and La which are larger than 1.42 Å are too large for the B sites. It should be noted that Fe is among the smallest atoms entering either site.

C. Band structure

The band-structure model of Switendick explains many of the features of Fe_3Si and its alloys. In order to produce a moment, this theory invokes an exchange splitting which transfers electrons at the Fermi energy from spin-down states to spin-up states. Because some d states of Fe(B) sites are above the Fermi energy and some d states of Fe(A,C) sites below it, charge transfer occurs and the moments on the two sites differ. Specifically two electrons per unit cell are transferred from the d bands of Fe(B) to those of Fe(A,C) sites. The change of Coulomb energy is compensated by exchange energy. Thus, the B sites are more positive than the A,C sites, providing suitable environments for atom cores such as Mn, which are less electronegative than Fe.

When Mn is substituted into Fe_3Si, d electrons are removed from the A,C sites and the redistribution of the electrons within the spin-up and spin-down subbands results in a reduced A,C moment. An extension of these calculations to substitutions further to the left, Cr, V, and Ti would require progressively greater charge transfers from the A,C sites and a decrease in the exchange splittings.

Predictions confirmed by magnetization measurements show that Mn enter Fe_3Si with a $\sim 2.2\mu_B$ moment while V and Ti enter with $\sim 0\mu_B$ moments.

Since the A,C sites are more negative they provide environments suitable for more electronegative elements like Co which have more electrons than Fe. On introducing Co the exchange splitting increases. Magnetization and neutron-diffraction results show that Co in the A,C site has a $1.7\mu_B$ moment and that the moment of Fe(B) atoms increase when these atoms have Co 1NN.[25] Alloys with Ni substitutions show the same general trends.

D. Electronic structure

Atoms to the right of Fe in the periodic table have good solubility in Fe_3Si up to Pd, Cu, Ag, and Au which are largely insoluble or cause at least one other phase to precipitate. The electronic structures of these atoms are $4d^{10}4s^0$, $3d^{10}3s^1$, $4d^{10}4s^1$, and $5d^{10}5s^1$ indicating a closed d shell. These electron configurations are for a free atom and of limited usefulness for an atom in a metal. They certainly indicate, however, that greater energies would be required to accomplish any interaction involving the d electrons of these atoms than with those of the other A,C site substitutions. The data on the change of the Fe(A,C) site's moments surely indicates changes involving d electrons at the A,C sites.

E. Comparison of Fe_3Si solute fields to those in Fe

The hyperfine fields of all the atoms now known to enter Fe_3Si are listed in Table IV. Also listed are the fields at the same nuclei in Fe metal. We note that most of these impurities have an internal field in Fe_3Si about 0.60 of their field in Fe. The only notable exceptions are the fields of Mn(B) and Fe(B), atoms with large local moments of about $2.2\mu_B$. Thus we believe that a reasonable estimate of the internal field of most atoms in Fe_3Si is 0.6 of its field in Fe.

The internal fields at V, Mn, Fe(B), Fe(A,C), and Si have been explained by the model described in Sec. V A 3. These fields, with the exception of the Fe(B) field, are changed from the value found in Fe because of changes in their on site moments and 1NN environments. The model also makes clear that Mn, V, and Si produce remarkably similar effects on their Fe(A,C) 1NN. The charge transfer effects produced by these substitutions result in changes of the magnetic moment of the substituted atom and also its 1NN atoms which in turn effect the on site and transferred internal fields.

As originally pointed out by Shirley and Westenbauger[26] the internal fields of most impurities in Fe, Co, and Ni vary almost linear with the moment of the host metals. The most inclusive treatment of this idea is by Balabanov[27] who offered an empirical formula which fits the hyperfine fields, H, of impurities in Fe, Ni, and Co matrices. Agreement with the data is generally good and does not exceed 20% in the worst cases. The Balabanov formula is

$$H = [-2.48 + 0.113(\nu - 9)^2]\mu / Z_0^{1.3} \ ,$$

where μ is the moment per atom of the matrix, Z_0 the number of electrons in filled shells, and ν the number of electrons in the partially filled shells. The constants -2.48 and 0.113 are obtained by fitting the equations to the data. The field at the nucleus obtained from the Thomas-Fermi model of the atom is proportioned to $Z^{1.3}$ and thus is essentially a measure of atomic size. Stearns[39] and Kagan[40] have also emphasized the role of an impurities size in computing its internal field.

Since the average host moment would be the same for all sites in Fe_3Si and since there are a variety of different fields in Fe(A,C) sites produced by strong 1NN interactions it is not possible to apply this formula in its present form in the impurities in Fe_3Si.

TABLE IV. Summary of metallurgical and hyperfine-field data for $Fe_{3-x}T_xSi$ alloys. The nuclear parameters and the internal fields of transition metals in Fe are included for purposes of comparison. The symbols employed in the table to designate the measuring technique used for the field values reported are hf—hyperfine field, M—Mössbauer, NMR—nuclear magnetic resonance cw or spin echo, NP—neutron polarization, PAC—perturbed angular correlation, NH—neutron diffraction, He—helium temperatures, and RT—room temperature. The new results reported for the first time in this note are indicated by pp (present paper).

Metallurgical data					Nuclear data				Internal fields: T in Fe					T in Fe_3Si $x \to 0$	
Element	Phases	Site occupied	Highest x	Ref.	Isotope	Natural abundance (at.%)	Gyromagnetic ratio (MHz/kG)	Nuclear spin	T (at.%)	Temp. (K)	hf (kG)	Method	Ref.	Temp.=1.4 K hf (kG)	Ref.
							3d metals								
Ti	Single	*B*	0.7[a]	2	47	7.52	0.2400	$\frac{5}{2}$							
					49	5.46	0.2401	$\frac{7}{2}$							
V	Single	*B*	1.0[a]	5	51	100	1.1193	$\frac{7}{2}$	4.4	4.2	87.1	NMR	28	47.7	5
Cr	Single	*B*	>1.0[a]	7	53	9.5	0.2406	$\frac{3}{2}$			−10(4)	PAC	15		
Mn	Single	*B*[b]	3.0[a]	7	55	100	1.0553	$\frac{5}{2}$	1	0	−227	NMR	29	258.9	7
Fe		*B* *A,C*			57	2.19	0.138	$\frac{1}{2}$		0	−336.9	NMR	30	338.5 218.4	8
Co	Single	*A,C*[c]	2.15[a]	25	59	100	1.0103	$\frac{7}{2}$	1	0	−287.7	NMR M	31	192.7	25
Ni	Single	*A,C*	0.8[a]	pp	61	1.25	0.379	$\frac{3}{2}$	1	77	234.2	NMR	32	159.89	pp
Cu	Fe_3Si		≈ 0	pp	63	69.1	1.1285	$\frac{3}{2}$							
	+Cu				65	30.9	1.2090	$\frac{3}{2}$							
							4d metals								
Nb	Fe_3Si +Fe_2Nb		≈ 0	pp	93	100	1.0407	$\frac{9}{2}$	<2	4.2	−258	NMR	29		
Mo	Fe_3Si		≈ 0	pp	95	15.9	0.2774	$\frac{5}{2}$	<2	4.2	−256	NMR	29		
	+Fe_2Mo				97	9.6	0.2833	$\frac{5}{2}$							
Ru	Single	*A,C*	0.25	1	99	12.72	0.19	$\frac{5}{2}$	2.3	4.2	500(10)	M	33	283.2	1
					101	17.07	0.21	$\frac{5}{2}$	2.5	4.2	504(1)	NMR	34		
Rh	Single	*A,C*	0.15	1	103	100	0.1340	$\frac{1}{2}$	<2	He	−543(11)	NMR	29	294	1
					100					0	559(1)	NMR	35		
Pd	Pd in Fe_3Si +Pd_2Si	*A,C*	0.25	pp	105	22.33	0.174	$\frac{5}{2}$	<2	He	−594(12)	NMR	36 29	336.2	pp
Ag	Fe_3Si		≈ 0	pp	107	51.4	0.1723	$\frac{1}{2}$	<2	4.2	−272	NMR	29		
	+Ag				109	48.6	0.1985	$\frac{1}{2}$							

							5d metals								
Ta	Fe_3Si $+Fe_2Ta$		≈ 0	pp	181	100	0.509	$\frac{7}{2}$	< 2	4.2	656	NMR	29		
W	Fe_3Si $+Fe_2Ta$		≈ 0	pp	183	14.3	0.175	$\frac{1}{2}$	< 2	4.2	643	NMR	29		
Re	Single	?	0.12	pp	185	37.07	0.9586	$\frac{5}{2}$	< 2	4.2	760	NMR	29		
					187	62.93	0.9684	$\frac{5}{2}$							
Os	Single	A,C	0.25	2	187	1.64	0.18	$\frac{1}{2}$							
					189	16.1	0.3307	$\frac{3}{2}$	< 2	He	1130(23)	NMR	29 37	728.8	1
Ir	Single	A,C	0.08	2	191	38.5	0.0813	$\frac{3}{2}$	< 2	He	1400(28)[d]	NMR	29 37	774.9[d]	1
					193	61.5	0.086	$\frac{3}{2}$							
Pt	Fe_3Si +second		≈ 0	pp	195	33.7	0.9153	$\frac{1}{2}$	< 2	4.2	1306	NMR	29		
Au	Au in Fe_3Si $+Au$	A,C	< 0.0025	pp	197	100	0.0731	$\frac{3}{2}$	< 2	4.2	1280	NMR	29		
							sp elements								
Al	Single	*D*	1	38	27	100	1.1094	$\frac{5}{2}$	2	4.2	−55	NMR	37	14.06	38
Si		*D*			29	4.7	0.8458	$\frac{1}{2}$						37.24	

[a]These values for x probably represent solubility limits.
[b]Detailed NMR measurements of $Fe_{3-x}Mn_xSi$ alloys with 0×1.6 show that Mn also enters the other two sites, namely, for x 0.75 Mn is found to enter the Fe(A,C) site. About 3% Mn occupies the Si sites at all compositions. The hyperfine fields for Mn in the Si and Fe(A,C) sites are 126 and 26 kOe, respectively.
[c]At higher compositions, Co also enters the Fe(A,C) sites (Ref. 25).
[d]Clear quadrupolar effects at the Ir site are seen in these alloys.

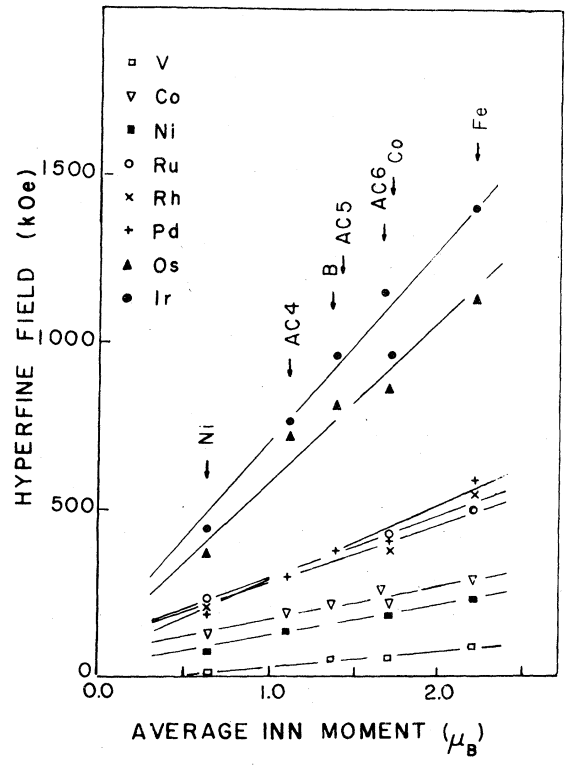

FIG. 17. Plot of internal field vs average first-near-neighbor moment for impurities in Fe, Ni, Co, and Fe_3Si.

The proportionality between the fields at Fe(A,C) sites and the average 1NN moment suggests a redefinition of μ to "the average moment of an atom's 1NN." In this form the agreement between the calculated and measured fields of elements substituted in Fe_3Si is as good as the agreement originally found for the fields at impurities Fe, Co, and Ni.

In Fig. 17 we plot internal field versus average 1NN moment for a number of nuclei in Fe, Co, Ni, and Fe_3Si.

We believe that the redefinition of the moment term in the Balabonov formula produces a more satisfactory equation since it extends the matrices to which the formula applies to long-range ordered alloys and compounds. Moreover, it provides a more accurate picture of the hyperfine interactions in ferromagnetic materials because in this new form the very local character of the hyperfine interactions is emphasized. The interactions of more distant neighbors may now be included in the moment term.

VII. CONCLUSION

The hyperfine-field measurements of the nuclei of transition-metal impurities have clearly shown that transition metals, in dilute concentrations, selectively occupy only one of the two inequivalent Fe sites in the Fe_3Si. The $3d$ metals to the left of Fe in the periodic table Mn, Cr, V, and Ti replace Fe in the B site and those to the right of Fe, Co, and Ni replace Fe in the A,C site. The $4d$ and $5d$ elements to the right and under Fe, Ru, Rh, Pd, Cs, and Ir also enter the A,C sites. Furthermore Ni and the $4d$ elements Ru, Rh, and Pd show an additional preference in nonstoichiometric alloys for the A,C sites with fewer Fe 1NN. The $4d$ and $5d$ elements to the left of Fe and the noble metals appear to be for the most part insoluble in Fe_3Si.

We conclude that electronegativity is an important factor in the site selection. The electronegativities of those atoms entering the A,C sites (1.8–2.2) are larger than those entering the B sites (1.5–1.6) indicating that the B site prefers atoms which can give electrons and the A,C site atoms which can receive electrons. This phenomonological conclusion derived from our data is similar to the conclusion of band-structure calculations on Fe_3Si.

We pointed out that by using the average 1NN moment rather than a matrix moment the dependences of internal fields on host moment and hyperfine-field systematics for impurities in ferromagnetic hosts can be extended to pseudobinary Fe_3Si alloys. Indeed the internal fields at V, Mn, Fe(B), Fe(A,C), and Si(D) were explained by a model which assumes that the transferred hyperfine field is owing principally to the exchange interaction with 1NN moments.

ACKNOWLEDGMENTS

Research done at the University of Connecticut was funded by the University of Connecticut Research Foundation. Research done at the Virginia Commonwealth University was funded by the Virginia Commonwealth University Research Foundation.

[1]T. J. Burch, T. Litrenta, and J. I. Budnick, Phys. Rev. Lett. 33, 421 (1974).
[2]S. Pickart, T. Litrenta, T. J. Burch, and J. I. Budnick, Phys. Lett. A 53, 321 (1975).
[3]T. Litrenta, Ph.D. thesis (Fordham University, 1975) (unpublished).
[4]V. Niculescu, K. Raj, T. J. Burch, and J. I. Budnick, Phys. Rev. B 13, 3167 (1976).
[5]V. Niculescu, K. Raj, J. I. Budnick, T. J. Burch, W. A. Hines, and A. H. Menotti, Phys. Rev. B 14, 4160 (1976).
[6]J. I. Budnick and S. Skalski, in *Hyperfine Interactions,* edited by A. J. Freeman and B. Frankel (Academic, New York, 1967), p. 724.
[7]W. A. Hines, A. H. Menotti, J. I. Budnick, T. J. Burch, T. Litrenta, V. Niculescu, and K. Raj, Phys. Rev. B 13, 4060 (1976).
[8]A. Paoletti and L. Passari, Nuovo Cimento 32, 1450 (1964).
[9]D. Meinhardt and C. Krisement, Z. Phys. 174, 472 (1963).
[10]J. I. Budnick, S. Skalski, T. J. Burch, and J. H. Wernick J. Appl. Phys. 38, 1137 (1967).
[11]M. B. Stearns, Phys. Rev. B 4, 4069 (1971); M. B. Stearns, L. A. Feldkamp, and J. F. Ullrich, Phys. Lett. A 30, 443 (1969).
[12]M. B. Stearns, Phys. Rev. 129, 1136 (1963).
[13]C. Blaauw, G. R. Mackay, and W. Leiper, Solid State Commun. 18, 729 (1976).
[14]S. Yoon and J. G. Booth, Phys. Lett. A 48, 381 (1974).
[15]S. A. Wedner, L. Keszthelyi, and J. A. Cameron, J. Phys. 57, 827 (1976).
[16]I. A. Campbell, J. Phys. C 2, 1338 (1969).
[17]Le Dang Khoi, P. Veillet, and I. A. Campbell, J. Phys. F 5, L203 (1975); 4, 2310 (1974).
[18]A. Parthasarathi and P. A. Beck, Solid State Commun. 18, 211 (1976).
[19]V. Niculescu, T. J. Burch, K. Raj, and J. I. Budnick, J. Magn. Magn. Mater. 5, 60 (1977).
[20]V. Niculescu and J. I. Budnick, Solid State Commun. 24, 631 (1977).
[21]L. Darken and R. W. Gurry, *Physical Chemistry of Metals* (McGraw-Hill, New York, 1953), pp. 86–89.
[22]K. Ono, Y. Ishikawa, and I. Ito, J. Phys. Soc. Jpn. 17, 1747 (1962).
[23]A. C. Switendick, Solid State Commun. 19, 511 (1976).
[24]P. Jenn and D. W. Geldart, Solid State Commun. 15, 139 (1974).
[25]V. Niculescu, J. I. Budnick, W. A. Hines, K. Raj, S. Pickart, and S. Skalski, Phys. Rev. 19, 452 (1979).
[26]D. A. Shirley and G. A. Westenberger, Phys. Rev. 138, A170 (1965).
[27]A. E. Balabanov and N. N. Delyagin, Sov. Phys. JETP 27, 752 (1968) [Zh. Eksp. Teor. Fiz. 54, 1402 (1968)].
[28]M. Rubinstein, G. M. Stauss, and J. Dweck, Phys. Rev. Lett. 17, 1001 (1966).
[29]M. Kontani and J. Itoh, J. Phys. Soc. Jpn. 22, 345 (1967).
[30]J. I. Budnick, L. J. Bruner, R. J. Blume, and E. L. Boyd, J. Appl. Phys. 32, 1209 (1961).
[31]J. G. Dash, R. D. Taylor, P. P. Craig, D. E. Nagle, D. R. F. Cochran, and W. E. Keller, Phys. Rev. Lett. 5, 152 (1960).
[32]R. L. Streever, L. H. Bennett, R. C. La Force, and G. F. Day, J. Appl. Phys. 34, 1050 (1963).
[33]Y. Koi, A. Tsujimura, T. Hihara, and T. Kushido, J. Phys. Soc. Jpn. 17, 96 (1962).
[34]J. J. Murphy, T. J. Burch, and J. I. Budnick, J. Phys. Soc. Jpn. 36, 634 (1974).
[35]O. C. Kistner, Phys. Rev. 144, 1022 (1966).
[36]J. I. Budnick, R. E. Gegenwarth, and J. G. Wernick, Bull. Am. Phys. Soc. II 10, 444 (1965).
[37]A. Stolovy, Bull. Am. Phys. Soc. 119, 461 (1964).
[38]T. J. Burch, K. Raj, P. Jena, J. I. Budnick, V. Niculescu, and W. B. Muir, Phys. Rev. B 19, 2933 (1979).
[39]M. B. Stearns, Phys. Lett. A 34, 146 (1971).
[40]A. V. Kogan, Sov. Phys. Solid State 9, 251 (1967) [Fiz. Tverd. Tela. 9, 336 (1967)].